

# Fourier Transform IR and Differential Scanning Calorimetry Study of Curing of Trifunctional Amino-Epoxy Resin

F. Carrasco,<sup>1</sup> P. Pagès,<sup>2</sup> T. Lacorte,<sup>2</sup> K. Briceño<sup>3</sup>

<sup>1</sup>Department of Chemical Engineering, Universitat de Girona, Avinguda Luis Santalo, s/n 17071 Girona, Spain

<sup>2</sup>Department of Material Science, Universitat Politècnica de Catalunya, Terrassa, Spain

<sup>3</sup>Department of Mechanical Engineering, Universidad Simón Bolívar, Baruta, Caracas, Venezuela

Received 4 August 2004; accepted 9 January 2005

DOI 10.1002/app.21978

Published online in Wiley InterScience (www.interscience.wiley.com).

**ABSTRACT:** The curing process was studied for a trifunctional epoxy resin, triglycidyl-*p*-aminophenol, using the hardener 4,4'-diaminodiphenylsulfone. Two curing cycles were carried out: one following the manufacturer's guidelines (2 h at 80°C, 1 h at 100°C, 4 h at 150°C, and 24 h at 200°C) and another proposed in this study, in which the two stages at low temperatures were excluded. Fourier transform IR spectroscopy was used to quantify the conversion of different functional groups (primary amine, secondary amine, epoxide, hydroxyl and ether functional groups), and these conversions could be used to infer the type of reactions that took place. These results allowed us to analyze the evolution of the curing process over time and the influence

of the curing cycle. Furthermore, the enthalpy of the curing process was determined using differential scanning calorimetry, and from this the thermal conversion for the whole process was evaluated. By taking into account the autocatalytic kinetic model, the rate constants were evaluated. The glass-transition temperatures were also estimated by applying different curing cycles to the resin. © 2005 Wiley Periodicals, Inc. *J Appl Polym Sci* 98: 1524–1535, 2005

**Key words:** curing; trifunctional epoxy resin; Fourier transform IR; differential scanning calorimetry; conversion of functional groups; overall thermal conversion; kinetic model; glass-transition temperature

## INTRODUCTION

Bifunctional resins, such as diglycidyl ether of bisphenol A (DGEBA), have been the most frequently used resins in different applications related to epoxy resins. However, 30 years after the first appearance of these bifunctional resins on the market, Dow Chemicals presented a new generation of multifunctional resins (degree of functionality = 3–5), which have had a great impact on the resin market since then because of their superior advantages compared to their predecessors. At the same curing degree, multifunctional resins have better crosslinking density and glass-transition temperatures than bifunctional resins.<sup>1</sup> Furthermore, they provide thermal, dynamic, mechanical, and adhesive improvements.<sup>2</sup>

Among the epoxy multifunctional resins, aromatic glycidyl resins and aromatic amino-glycidyl resins stand out. A trifunctional epoxy resin derived from *p*-aminophenol was developed by Ciba-Geigy, and it is extensively used as an adhesive and in structural applications. Moreover, it has a low viscosity (0.5–2.5

Pa s), allowing curing at relatively low temperatures (e.g., at 70°C), and it develops excellent properties at high temperatures.

One of most common ways of curing epoxy resins involves the use of curing agents, which are capable of interlinking the resins' chains. The main agents are primary and secondary amines as well as dibasic acids or acid anhydrides.<sup>3</sup> The reactivity of some commercial epoxy resins has been increased by the presence of ether bonds that, even when separated from the epoxide ring by the methylene group, have a great activating effect on the epoxide group. Because of this reactivity, the epoxide groups can be opened not only by available ions and active hydrogens but also by tertiary amines. Each primary amine group is theoretically capable of reacting with two epoxide groups. In the case of bifunctional resins, it is expected that the epoxide group is opened by the primary amines. When the remaining secondary hydrogen combines with a new epoxy molecule, a branch point is formed. The rate at which the branching or the linear growth of the polymer occurs depends on the relative rate of the epoxide group with the hydrogens of the primary or secondary amines. The volume contraction that takes place during the curing process is the result of the formation of covalent bonds where there are bonds formed by van der Waals forces. Furthermore, this

Correspondence to: F. Carrasco (felix.carrasco@udg.es).

increases the glass-transition temperature because of the increase in the molecular agglomeration.<sup>4</sup>

We consider three reactions for curing amino-epoxy resins: reaction of the epoxide group with primary amines, in which an N—C bond is formed and a hydroxyl group appears that is also reactive; reaction of the epoxide group with secondary amines, with the consequent formation of a new N—C bond and the appearance of a new hydroxyl group; and etherification of the epoxide group with the hydroxyls generated in the previous reactions. This reaction causes the appearance of an ether bridge.<sup>5</sup> In general, the reactions for curing multifunctional resins are more complex than those for bifunctional resins.

The study of side reactions has been a point of interest because they influence the formation and properties of the structural network. These reactions can take place in either the presence or absence of curing agents (initiators or catalysers), depending on the degree of functionality of the epoxy resin, and can be quantified by measuring the conversion ratio between the epoxide and amine groups. Bonnaud et al.<sup>6</sup> have also observed etherification reactions, although only at high temperatures.

Vitrification has been observed in many DGEBA resins because, when the glass-transition temperature reaches the curing temperature, the resin undergoes vitrification and the mobility of the molecules is reduced. From this point on, the curing process proceeds thanks to diffusion and the glass-transition temperature ceases to increase significantly. However, in triglycidyl-*p*-aminophenol (TGAP) resins, the glass-transition temperature continues to increase after vitrification with the curing temperature, probably because of their higher functionality (i.e., there are more reactive sites). In this case, when the resin undergoes vitrification, not only etherification reactions take place but also other intermolecular reactions.<sup>6</sup>

The reaction mechanism and the kinetics of the curing process for an epoxy resin determine the morphology of the 3-dimensional network, thus defining its physical and mechanical properties. Numerous kinetic studies on epoxy resins have been carried out and quite a few unanswered questions and certain contradictions have been found; for this reason, there is still interest in this subject.<sup>7–10</sup> There are two types of kinetic models: mechanistic and phenomenological. The mechanistic models are extremely complex because they imply identifying the elemental reactions and determining which of them is the rate-determining step. Because of this, researchers have opted for the phenomenological models in order to study the curing process of thermoset materials. Although these models do not supply information about the network formation process, they are very useful because they allow the overall rate of the process to be quantified, a variable that is fundamental in order to design the

curing process reactor. The kinetic models most widely used are the *n*-order, autocatalytic, and diffusion controlled. The *n*-order kinetic model is frequently employed for all types of reactions because of its simplicity (although it is widely known that it only has scientific foundation in reactions in the gaseous phase). However, the global curing process does not usually follow this type of model, even though a good fit to the experimental data has been observed in the case of curing bifunctional DGEBA resins with anhydride.<sup>9</sup> The autocatalytic kinetic model has been very successful in curing amino-epoxy resins.<sup>5,11–16</sup> In the self-catalytic curing reactions, one of the reaction products carries out the role of catalyst, accelerating the reactions. However, this model does not usually provide good fits at high conversions because, in these conditions, in which the glass-transition temperature of the network reaches the operation temperature, the curing process is controlled by diffusion.<sup>12</sup> This confirms the complexity of the reactions involved in the overall curing process.

To follow the reactions that take place in the curing process, Fourier transform IR spectroscopy (FTIR) is a very useful tool because it allows the quantification of the concentration of the epoxide, hydroxyl, and ether groups, as well as primary, secondary, and tertiary amines.<sup>2,7,11,17–19</sup> It is also possible to follow complex reactions such as cyclization and etherification.<sup>20</sup> Differential scanning calorimetry (DSC) is also a very useful technique, given that the global enthalpy of the process can be determined from the thermograms and from this the overall thermal conversion. Furthermore, the glass-transition temperature can be evaluated.

The aim of this article was to follow the appearance and disappearance of functional groups throughout the curing process by means of FTIR for trifunctional TGAP resins, using two curing cycles (one established by the manufacturers and the other proposed in this study). The overall curing conversion and the glass-transition temperature were also evaluated by DSC.

## EXPERIMENTAL

### Materials

The resin that was used was a trifunctional epoxy resin called TGAP (Araldite MY 510, Ciba-Geigy). Its physical properties are 0.55–0.85 Pa s viscosity at 25°C, 1205–1225 kg/m<sup>3</sup> density at 25°C, and 0.20% maximum water content.

The hardener in the study was a diamine called 4,4'-diaminodiphenylsulfone (HT-976-1, Ciba-Geigy). Its physical properties are 1300 kg/m<sup>3</sup> density at 25°C, 176–185°C melting temperature, 99–100% amine content, and 0.15% maximum water content.

## Curing process

A resin/hardener mass ratio of 100 : 52 was used. This mass ratio corresponds to a 1 : 0.9 epoxy/amine molar ratio. A slight excess of epoxy is generally used in this type of resin because, if an epoxy/amine stoichiometric ratio is used, many of the remaining functional groups fail to react because of spatial entrapment in an immobile, rigid epoxy network. Excess amine in a cured composite serves only to further aid moisture ingress and decrease the mechanical properties of the polymer. Thorough mixing of both materials was carried out in an aluminum receptacle submerged in a glycerine bath. The temperature was strictly controlled in the range of 60–80°C. The mix was agitated at low speed to minimize the formation of bubbles, the presence of which was practically negligible after 30 min of agitation.

The curing process was carried out using two different cycles:

1. Cycle 1: The curing process followed the manufacturer's instructions: the first stage is 2 h at 80°C, the second stage is 1 h at 100°C, the third stage is 4 h at 150°C, and the fourth stage is 24 h at 200°C.
2. Cycle 2: This consisted of carrying out the curing process by eliminating the first two stages at low temperature of cycle 1, by which 3 h of process time are saved. Therefore, cycle 2 is 4 h at 150°C in the first stage and 24 h at 200°C in the second stage.

## FTIR study

Characterization of the curing process for an amino-epoxy resin can be carried out in different ways. The most classical procedures are solvent swelling and titration of functional groups as the reaction proceeds. However, FTIR is a very useful tool because it allows the determination of the concentrations of all the functional groups involved in the curing process. The curing of this type of resin has been studied by near IR.<sup>11,21–23</sup>

For the spectroscopic tests, a thin layer of the sample was poured onto a smooth surface of NaCl, which is considered to be an appropriate support because it is inert to IR radiation within the range of this study and because it is stable at the temperatures of the curing process. The equipment used was a Nicolet 510 type spectrophotometer with CsI optics, and scanning was performed within a wavenumber interval of 4000–600  $\text{cm}^{-1}$ . The characteristic bands that were studied appear in Table I. These bands were previously used by other authors.<sup>24–27</sup> The variation in the absorbance of a particular band allowed the progress of the reaction to be quantified, having defined the conversion as  $\alpha$

**TABLE I**  
Characteristic Bands Related to Amino-Epoxy Resin

Wavenumber ( $\text{cm}^{-1}$ )	Functional group
3600–3200	OH (hydroxyl)
3472	NH <sub>2</sub> (primary amine)
3395	NH (secondary amine)
3380	NH <sub>2</sub> (primary amine)
3236	NH <sub>2</sub> (primary amine)
3038	C—H (in the epoxide group)
2998	C—H (in the epoxide group)
1629	NH <sub>2</sub> (primary amine)
1513	Aromatic ring
1292	OH (hydroxyl, ether)
1100	C—O—C (ether)
906	C—O—C (in the epoxide group)
692	N—H (primary amine)
642	N—H (primary amine)

$= 1 - A^*(t)/A^*(0)$ , where  $A^*(t)$  is the reduced absorbance after a certain time  $t$  and  $A^*(0)$  is the reduced absorbance at the start of the curing process. The  $A^*$  is used to correct for the thickness of the sample and consisted of dividing the absorbance of the band by the absorbance of an invariant band during the curing process. The absorbance at 1513  $\text{cm}^{-1}$  (stretching of the aromatic ring) was taken as an invariant band because this chemical group is not modified during the curing of the resin. We conducted the curing of the resin during 24 h and measured the absorbance at 1513  $\text{cm}^{-1}$ . (A correction was made in order to take into consideration the film thickness according the Lambert–Beer law.) The results indicated that the absorbance was constant and independent of the curing time. This band has been widely used as a standard band in previous works.<sup>27,28</sup>

## DSC study

DSC provides supplementary information that is very interesting because it allows the enthalpy of the process to be determined, from which the overall thermal conversion of the curing process can be quantified. It is also possible to evaluate the glass-transition temperature from the thermogram. In the tests 2–2.5 mg of the uncured sample was placed in a hermetically sealed aluminum boat, which was then placed in a calorimeter in which isothermal and dynamic experiments were carried out. An initial dynamic heating process was performed to heat the sample from 30 to 300°C at a rate of 10°C/min. This temperature was maintained for 1 min, after which the sample was cooled to 30°C at a rate of 10°C/min. Then, a second dynamic scanning was performed in order to determine the glass-transition temperature, which involved heating the sample from 30 to 300°C at 10°C/min. It is important to keep in mind that in the first heating

process it is not possible to observe the glass-transition temperature because of the gelation and crosslinking produced in this stage. After cooling and then reheating, it is then possible to observe this temperature, at which the segmental movements of the polymeric chain take place. In contrast, both isothermal experiments were carried out at 150 and 180°C during 4 h. The sample was cooled to 30°C at 10°C/min and was maintained at this temperature for 1 min, and then a dynamic heating process was performed bringing the temperature to 300°C at 10°C/min.

## RESULTS AND DISCUSSION

As mentioned in the Experimental section, the treatment at 200°C was performed during 24 h, as recommended by the manufacturer. However, after 7 h the primary amines in the hardener and epoxide groups of the resin had been almost completely consumed. For this reason significant differences were not observed in the bands corresponding to these functional groups between 7 and 24 h, which indicates complete curing from 7 h onward.

Figure 1 shows the FTIR spectra in the 4000–2500  $\text{cm}^{-1}$  interval for both types of curing cycles. Note that little differences existed in the wavenumbers between cycle 1 [Fig. 1(a)] and cycle 2 [Fig. 1(b)], but they were generally  $<0.2\%$ . The data showed the disappearance of the characteristic symmetrical and antisymmetrical stretching bands of the primary amine group at 3471 and 3373  $\text{cm}^{-1}$ , as well as a distinctive band of this functional group at 3242  $\text{cm}^{-1}$ . After 3 h at 200°C a characteristic band of secondary amines appeared at 3399  $\text{cm}^{-1}$ , considerably reducing the bands corresponding to the primary amine. From these observations it can be affirmed that the reaction in the first stages of the curing process was the disappearance of primary amine functional groups, with the subsequent appearance of secondary amine groups. Although it has already been established that the generation of secondary amine groups begins from the first stages of the primary amine reaction, this band was not observable in the corresponding spectra in the first hours of the curing process. This is probably due to the fact that the hydrogens of the secondary amines are 2–3 times less reactive than the hydrogens of the primary amines in aromatic amines (such as 4,4'-diaminodiphenylsulfone), a phenomenon different from that occurring with aliphatic amines, in which the hydrogens in the primary and secondary amines are similarly reactive.<sup>5</sup> The presence of the secondary amine after the third hour at 200°C when curing cycle 1 was applied [Fig. 1(a)] did not seem to be observable when curing cycle 2 was applied [Fig. 1(b)]. This phenomenon could be because in cycle 2 the band of the hydroxyl group appears earlier than it does in cycle 1, which can cause the amine and hydroxyl bands to

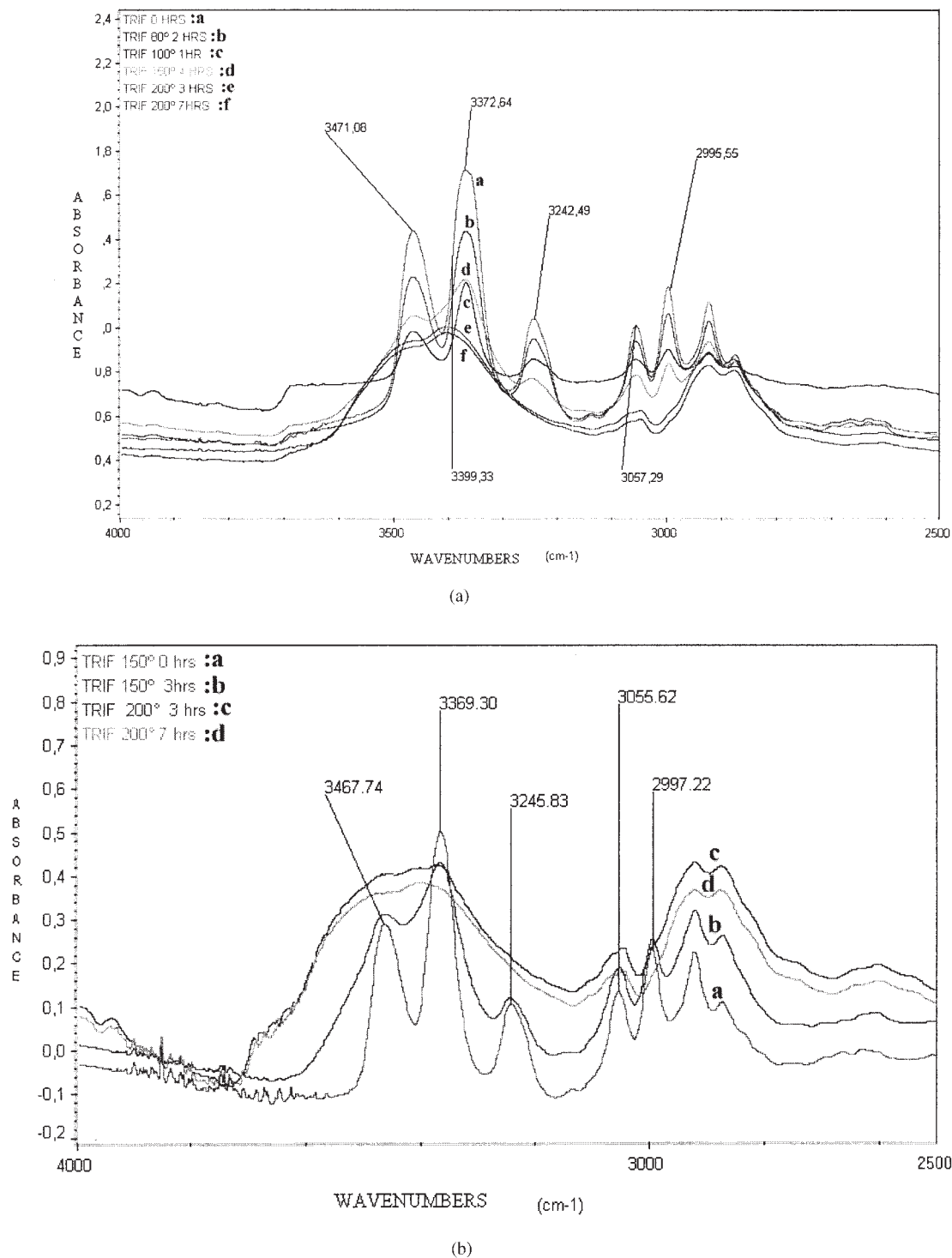
overlap. The appearance of a large, enveloping band between 3600 and 3000  $\text{cm}^{-1}$  can be seen in both cycles, which has been previously observed by Xiao et al.,<sup>7</sup> and is a characteristic of the tension in —OH and —NH groups. The above-mentioned enveloping appeared in a wide interval of wavenumbers, which has been considered as evidence of the existence of a large variety of chemical species that favor the formation of intermolecular hydrogen bonds.<sup>29</sup> The absorbances at 3057 (tension of the —CH group of the epoxide ring) and 2996  $\text{cm}^{-1}$  (stretching of the —CH<sub>2</sub> of the epoxide ring) decreased with time in both cycles of the curing process, which confirms the epoxide ring was opened as the reaction proceeded.

Figure 2 illustrates the spectra in the 1800–1000  $\text{cm}^{-1}$  zone for the two curing cycles studied. The absorbance of the band at 1631  $\text{cm}^{-1}$ , corresponding to the bending of the primary amine, decreased in both curing cycles. However, this decrease occurred earlier when cycle 2 was used, which corroborates the effect of the temperature. The band at 1295  $\text{cm}^{-1}$  corresponds to the —CH<sub>2</sub> groups in the ether, appearing from the beginning in curing cycle 2, and from the first hour at 100°C in curing cycle 1. This band remained throughout the whole curing process, and it should allow the proportion of ether groups present in the resin to be determined. However, this band was influenced by the hydroxyl group and therefore a precise quantification was not possible, even though it is known that etherification is one of the most important secondary reactions in curing amino-epoxy resins. This band could be supported by the appearance of bands that are characteristic of the asymmetrical stretching of C—O—C at 1075 and 1149  $\text{cm}^{-1}$ , as previously reported in the literature.<sup>27</sup>

Figure 3 illustrates the spectra in the 1000–600  $\text{cm}^{-1}$  zone for the curing cycles in the study. The absorbance at 696 and 649  $\text{cm}^{-1}$ , corresponding to the primary amines, decreased over the curing process and tended to disappear in both cycles when 200°C was reached, which corroborates the previous analyzed results. The spectra also highlighted the total disappearance of the band at 909  $\text{cm}^{-1}$  after 3 h of curing at 200°C for both cycles. This implies the complete disappearance of the epoxide groups as a consequence of the addition reactions with the primary and secondary amines. After 24 h at 200°C the bands corresponding to these functional groups were not detected.

The results presented up to now indicate that there is a wide range of spectral bands that could contribute to the study of the curing process. With the aim of establishing whether differences exist between the two curing cycles that we studied, it was necessary to quantify the rates of appearance and disappearance of the functional groups. This was possible by evaluating the conversion of each of these reactions. Figure 4 shows the conversion of the primary amines as a





**Figure 1** FTIR spectra in the 4000–2500 cm<sup>-1</sup> region of the cured resin in (a) cycle 1 and (b) cycle 2.

function of time for both curing cycles, taking into account different absorption bands of this functional group. In the initial part of the curing process, conversion of the primary amine groups was lower when employing cycle 1 (in which this period corresponds to much lower temperatures). At the end of 2 h, the primary amine conversion, established by the band at

3472 cm<sup>-1</sup> [Fig. 4(a)], was 6% for cycle 1 (at 80°C) and 36% for cycle 2 (at 150°C). This indicates that temperature has an important influence on the primary amine reaction during the first stages of the curing process. Taking into account the band at 3380 cm<sup>-1</sup> [Fig. 4(b)], the conversion at the end of 2 h was 1 and 24% for cycles 1 and 2, respectively, which indicates

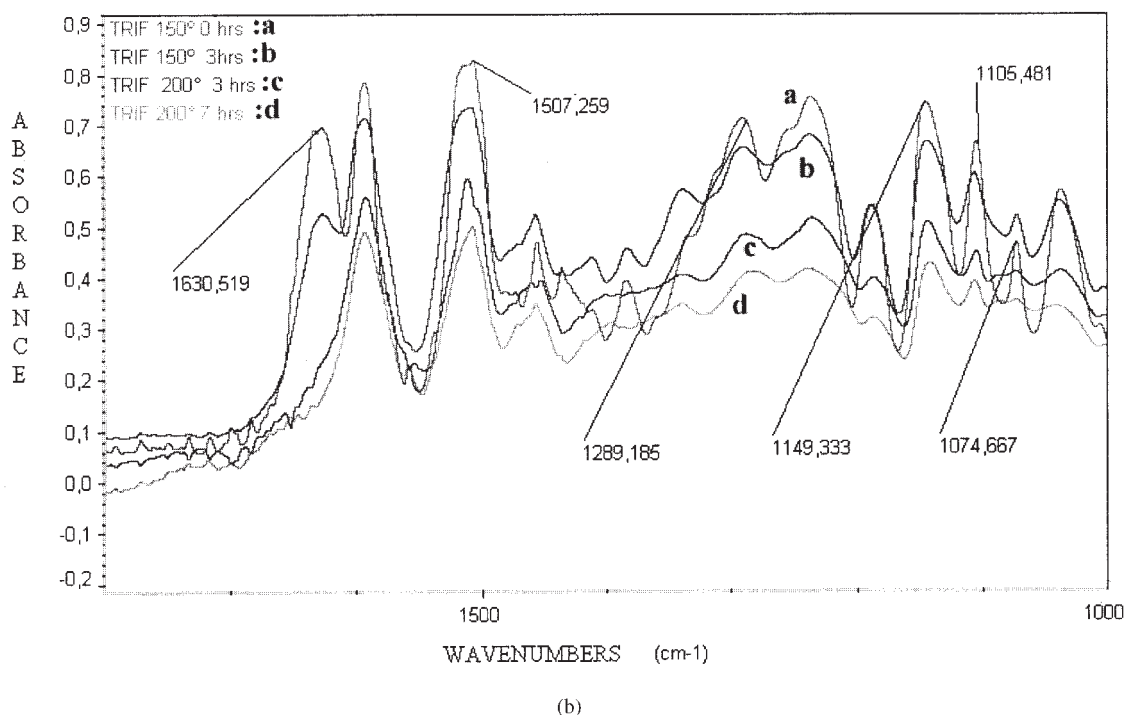
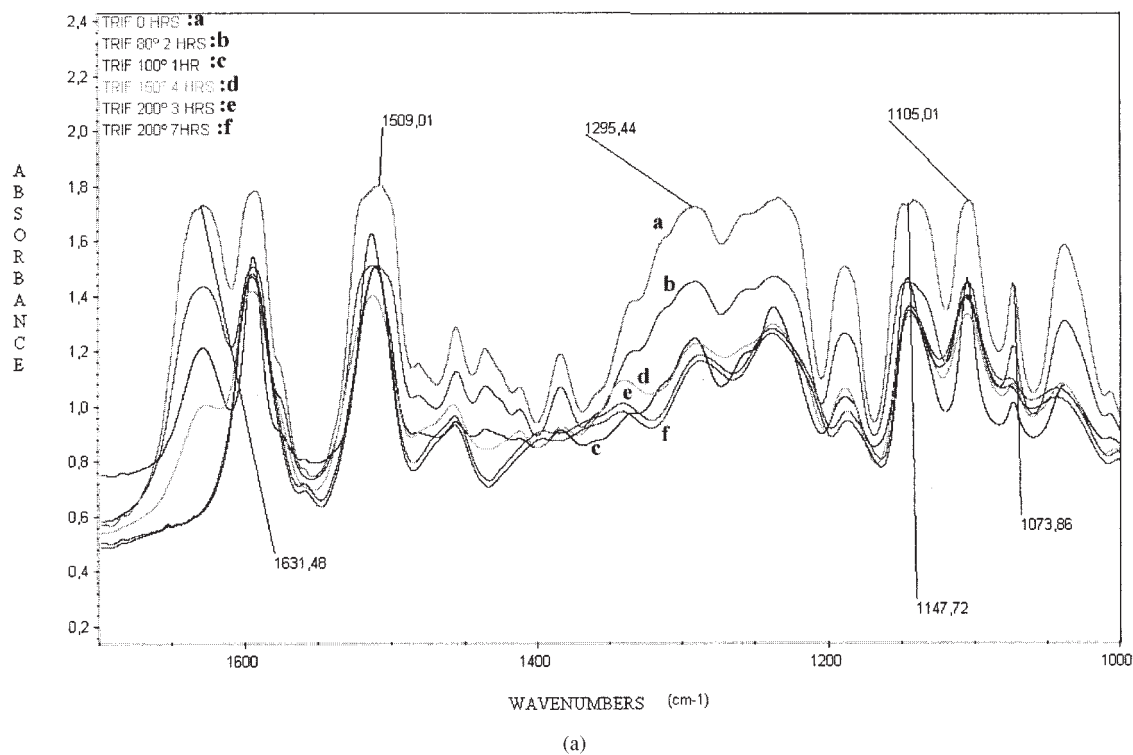
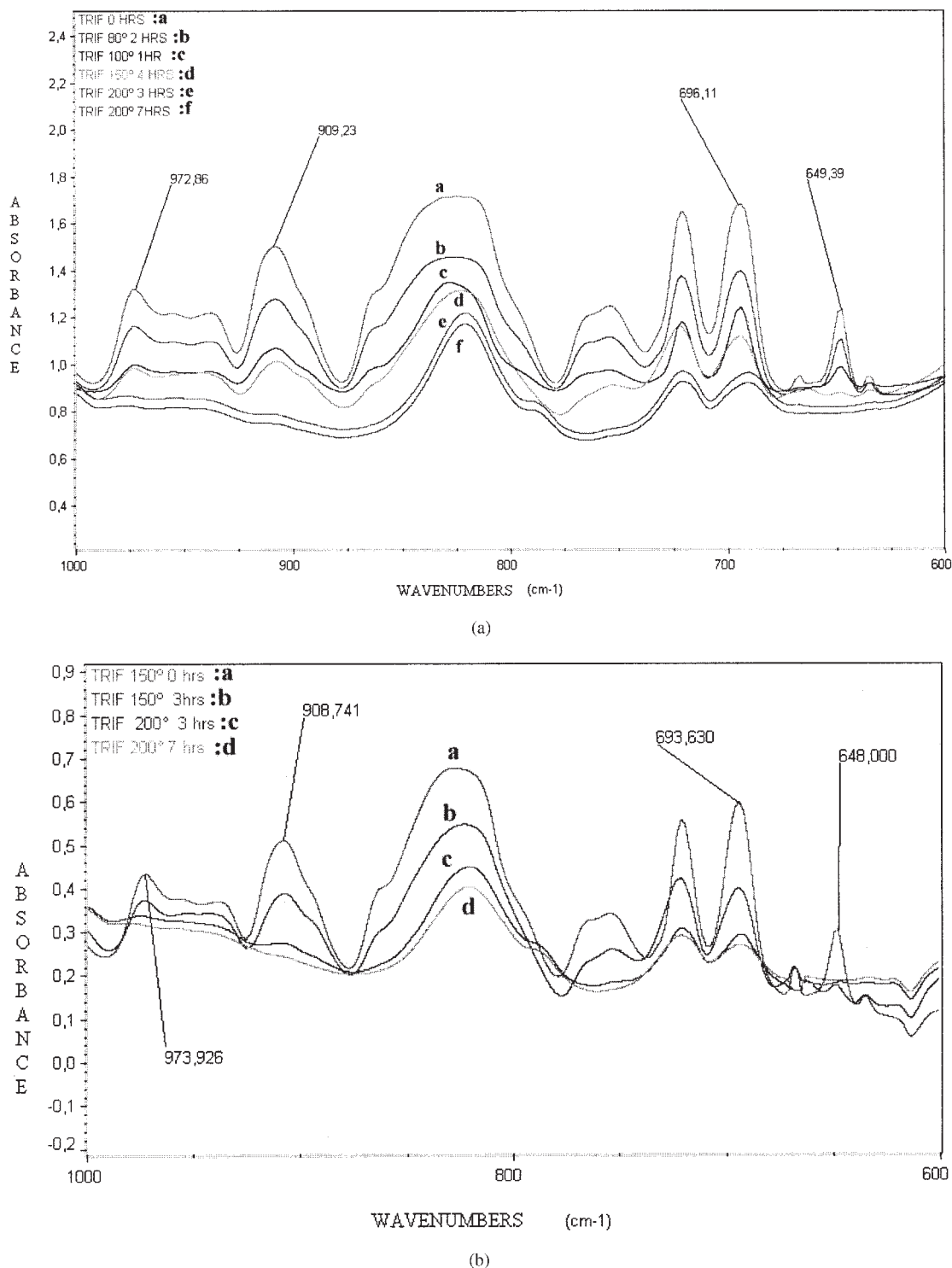


Figure 2 FTIR spectra in the 1800–1000  $\text{cm}^{-1}$  region of the cured resin in (a) cycle 1 and (b) cycle 2.

that the results obtained through the absorbances of asymmetric and symmetric tension in the  $\text{—NH}_2$  group followed a similar evolution. Analogous results were obtained by following the progress of the band at 1630  $\text{cm}^{-1}$  [Fig. 4(d)]; however, the differences between the two cycles are not very noticeable (conver-

sions of 14 and 27%). Although the influence of the temperature was very noticeable in the first 2 h (at 80°C in curing cycle 1 and 150°C in curing cycle 2), this lessened as time passed, in such a way that conversions obtained after 9 h of cycle 1 (i.e., 2 h at 80°C, 1 h at 100°C, 4 h at 150°C, and 2 h at 200°C) were similar



**Figure 3** FTIR spectra in the 1000–600  $\text{cm}^{-1}$  region of the cured resin in (a) cycle 1 and (b) cycle 2.

to those obtained after 4 h of cycle 2 (4 h at 150°C). The conversions obtained after finishing cycles 1 and 2 were 53 and 48 (band at 3380  $\text{cm}^{-1}$ ), 79 and 76 (band at 3245  $\text{cm}^{-1}$ ), and 66 and 80% (band at 1630  $\text{cm}^{-1}$ ). These results clearly indicated that there was little difference between the two curing sequences in the previously described conditions. Furthermore, the

conversions were very similar for the bands at 3245 and 1630  $\text{cm}^{-1}$  (mean value = 76%).

It is known that the curing mechanism of this type of epoxy resin is dominated by a first stage in which the primary amines disappear, which occurs fundamentally during the gelation stage of the resin. This implies that, before the gelation point is reached, a

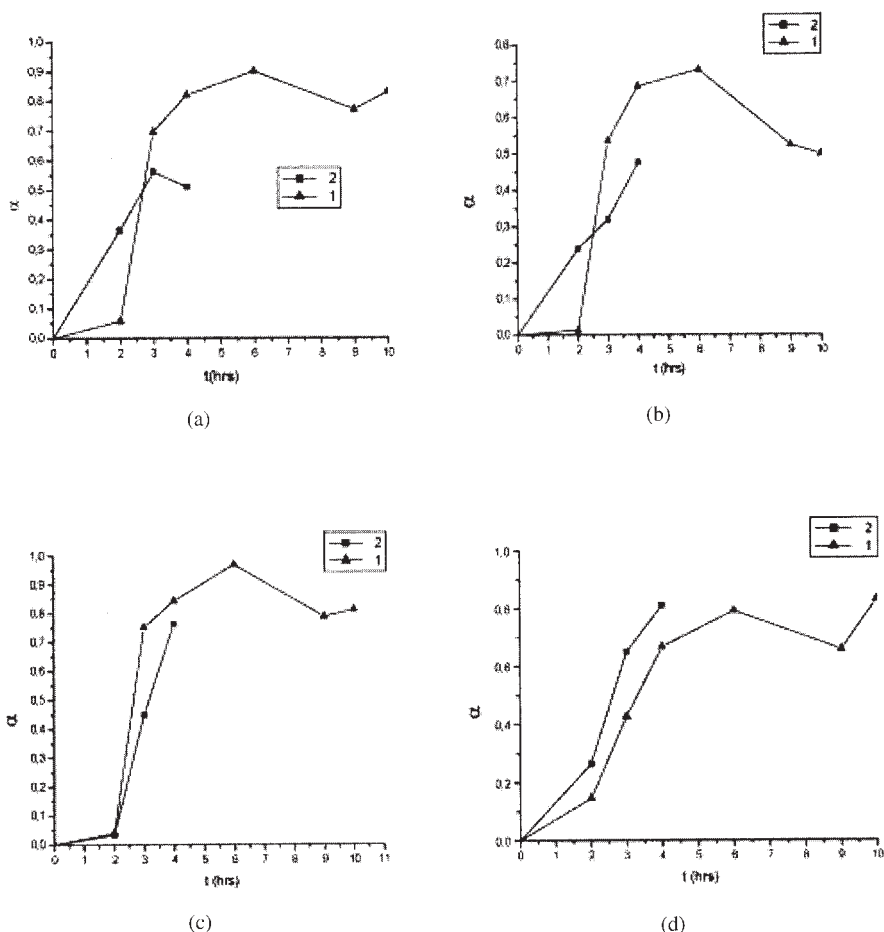


**Figure 4** The variation of the conversion of the primary amine versus time in the curing process at absorption bands of (a) 3471, (b) 3373, (c) 3242, and (d) 1631  $\text{cm}^{-1}$ .

type of linear polymerization is established that later gives rise to the intervention of secondary amines, which are responsible for branch reactions with the consequent formation of crosslinks. According to Varley et al.,<sup>23</sup> gelation of a resin with similar characteristics to the one studied in this work was independent of temperature, which could explain the similarity between the conversion values reached at the end of each curing stage of the two cycles under study (9 h in cycle 1 and 4 h in cycle 2). Therefore, the conversion of the primary amines is practically independent of the temperature–time sequence that was applied until the moment in which the 3-dimensional network begins to form, which takes place when the gelation of the resin occurs. This would also indicate that the primary amine reaction with the epoxide group would not be affected by viscosity during the gelation, in the stage called the sol fraction.<sup>11</sup> However, the reaction rate needed to reach these conversion values depended on the curing cycle applied, as inferred from the slopes of the plot of conversion versus time. It is important to keep in mind that curing trifunctional resins is more complicated than the process for bifunctional resins.

The presence of tertiary amines in the chemical structure of the epoxy molecule catalyzes the etherification reactions, which are very sensitive to temperature and have a significant influence on the evolution of the curing process.<sup>30</sup>

The evolution of the curing process can be determined by studying the variation of the number of hydroxyl groups, because they participate in the epoxy–amine addition reactions and are also catalysts for the curing process.<sup>23</sup> However, the presence of such a functional group, in a wavenumber interval where bands characteristic of primary and secondary amines appear, makes studying and later analyzing it extremely difficult, as already reported by Min et al.<sup>31</sup> In contrast, it is plausible to think that it would be useful to study the evolution of the band at 1105  $\text{cm}^{-1}$ , corresponding to the ether group C—O—C, in order to study the etherification reactions throughout the curing process. However, the results obtained were different than what was expected (i.e., an increase in the presence of ether groups) and therefore this band must be rejected to study the curing process.



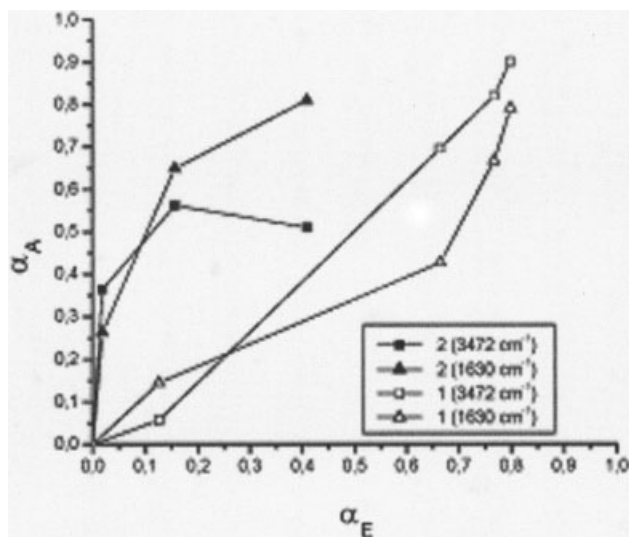


**Figure 5** The variation of the conversion of the primary amine versus the conversion of the epoxide group for the two curing cycles.

To analyze the influence of the curing cycle more easily, the conversion of the primary amine versus the conversion for the epoxide group was plotted (see Fig. 5). The results showed that, when curing cycle 1 was applied, the consumption of epoxide groups and amine groups was quite similar (especially for the band at  $3472\text{ cm}^{-1}$ ), which indicated that there was a nearly stoichiometric reaction between both functional groups. This was not true when cycle 2 was applied (i.e., higher temperatures because the stages at low temperatures were eliminated), given that the disappearance of primary amine groups was significantly different than the disappearance of epoxide groups. Even though the epoxide groups react with the primary amines from the beginning of the curing process, a lower proportion of secondary amines (product of the initial reaction) can compete with the primary amines, leading to new addition reactions with the epoxide groups. As reported by Gupta et al.,<sup>32</sup> addition is not the only reaction that takes place in these types of resins. In fact, the presence of voluminous groups could provoke steric hindrance when close to secondary amines, which would reduce the reaction rate of the hydrogens close to them, from which it can be inferred that other reactions must exist that are responsible for the consumption of epoxide groups. The etherification reactions for curing multifunctional epoxy resins are influenced by catalyst factors, like the presence of tertiary amines or the temperature. The rate of etherification is hardly affected during gelation in most bifunctional resins, so that the reaction between the secondary amine and the epoxide groups and the etherification become more important in the vitreous stage. However, it has been reported that, for trifunctional resins, these reactions start to be impor-

tant before arriving at the vitreous stage and they are also influenced by the temperature.<sup>23</sup> Thus, it is plausible to think that the disappearance of epoxide groups (as well as amine groups) tends to be greater in curing processes at higher temperatures for trifunctional resins (i.e., higher reaction rate). According to Xu and Schlup,<sup>20</sup> etherification can change the structure and, as a consequence, the thermal and mechanical properties when increasing branching points. At high temperatures, there is more competition between branching growth (due to etherification reactions) and the ether groups that do not react (i.e., that became entrapped), making the resin more fragile, given that there are more branches and less anchoring points.<sup>23</sup>

Figure 5 also illustrates the influence of temperature on the mechanism of curing reactions, so that, apart from the main reaction between amine and epoxide groups, there are other reactions that lead to conversions different from those expected when only the amine–epoxide reaction was considered. The differences observed in the conversions could be attributed to the removal of the low temperature stages in curing cycle 2. Effectively, in this curing cycle the hardener practically reached its melting point from the initial stages and consequently possessed greater reactivity and mobility, leading to a higher consumption capacity of the primary amine groups. By contrast, instability of the ether groups at higher temperature (i.e., cycle 2) can cause additional consumption of primary amine groups. The low temperature stages in curing cycle 1 led to a more sequential and moderated reaction for the hardener. Kim and Inoue<sup>33</sup> reported that the conversion of amine groups was also higher (as in our work) than that of epoxide groups when curing a thermoset/thermoplastic blend.

When the samples are subjected to DSC through isothermal scanning, certain types of reactions are unavoidable during the heating period before reaching the curing temperature. This means that the baseline changes before arriving at this temperature. For this reason, the baseline was estimated by taking into account the completely cured resin. Dynamic scanning was also carried out, in which the temperature increased at a constant heating rate. In all cases, the area below the heat flow curve allowed the total enthalpy of the curing process to be determined. By means of dynamic scanning at  $10^\circ\text{C}/\text{min}$  (the initial sample being the uncured resin), a total enthalpy of  $857\text{ J/g}$  was obtained, a greater value than those obtained with other epoxy resins, which were  $102$ ,  $667$ , and  $699\text{ J/g}$  for bifunctional,<sup>34</sup> trifunctional,<sup>32</sup> and tetrafunctional<sup>35</sup> epoxy resins, respectively. These results are possible because the enthalpy depends on the temperature, the type of experiment (isothermal or dynamic), and the type of resin. As the result of a second dynamic scanning, it was possible to determine the glass-transition temperature, estimated at  $220^\circ\text{C}$ , a key value to ex-

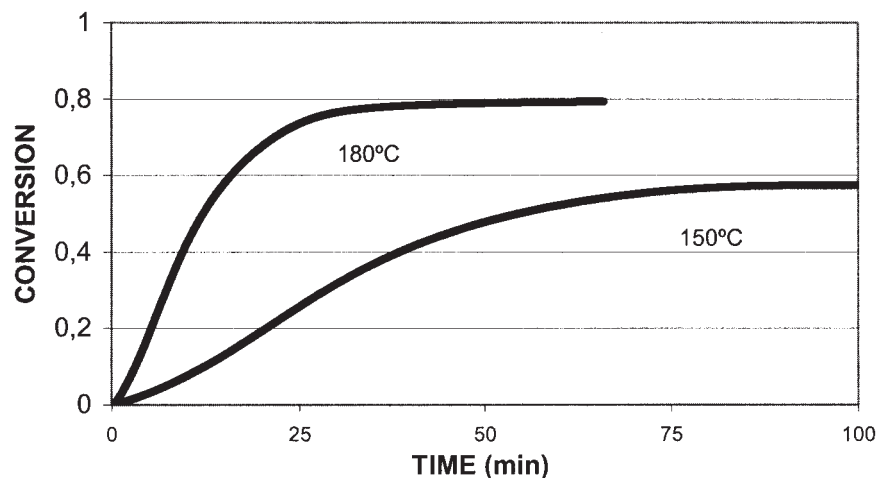


**Figure 6** The variation of the overall thermal conversion of the curing process determined by DSC at different temperatures (150 and 180°C).

plain the physical phenomena that occur during the curing process. Isothermal scanning was also carried out at 150 and 200°C, obtaining total enthalpies of the curing process of 553 and 741 J/g, which demonstrates the great influence the temperature has on the exothermic character of the reactions that take place during the curing process (i.e., higher temperature, greater exothermic character). These results are supported by Xiao et al.<sup>7</sup> who reported that epoxide-amine reactions are more exothermic than epoxide-hydroxyl ones, especially at high temperatures. After isothermal scanning, dynamic scanning was carried out at 10°C in order to observe the vitrification of the resin. The glass-transition temperatures were 200 and 220°C when the curing temperatures were 150 and 180°C, respectively. Again, the curing process at higher temperatures provided higher glass-transition temperatures.

Another useful aspect of DSC is that it allows the thermal conversion of the global curing process to be calculated as follows:  $\alpha = 1 - \Delta H_{nc} / \Delta H_{pc}$ , where  $\Delta H_{nc}$  is the enthalpy of the uncured resin and  $\Delta H_{pc}$  is the enthalpy of the partially cured sample at time  $t$ . Figure 6 illustrates the variation of the overall thermal conversion of the curing process as a function of time. Both curves (150 and 180°C) indicated that the rate of the curing process was initially higher and decreased as time passed, which is logical given that the proportion of available reactants also decreased. Furthermore, this initial rate was higher at 180 than at 150°C. The thermal conversion reached an asymptotic value:  $\alpha = 0.79$  at 180°C and  $\alpha = 0.57$  at 150°C. Thus, the maximum thermal conversion was greater at higher temperatures, and in both cases it was lower than 100%, which is evidence of the effect of vitrification. Other authors arrived at similar conclusions.<sup>14,23,36</sup> They reported that increasing the temperature in-

creased the conversion of the epoxy resin and it was not possible to arrive at 100% conversion because of the vitrification of the reaction mass. It is important to take into account that curing reactions progress according to different stages. In the first place, the curing process is conditioned by the activity of the reactive chemical groups and takes place in the liquid state. The moment arrives in which vitrification is initiated, at which point the reaction rate decreases considerably until it stops when the mobility of the reactive groups is very restricted. When the vitreous state is reached, the chemical reactions are controlled by diffusion and the only movements allowed are those due to structural relaxation. For this reason, it is impossible to reach complete conversion of the curing reactions.<sup>37</sup> The vitrification point is related to the inflexion point of the curve conversion versus time. As expected, vitrification was reached earlier when operating at higher temperatures, which corroborates the results in the literature related to curing similar resins.<sup>37</sup>

The autocatalytic kinetic equation is as follows:

$$r = \frac{d\alpha}{dt} = (k_1 + k_2\alpha^m)(1 - \alpha)^n \quad (1)$$

where  $r$  is the reaction rate ( $s^{-1}$ ),  $\alpha$  is the overall thermal conversion,  $k_1$  is the kinetic constant for the nonautocatalytic reaction ( $s^{-1}$ ),  $k_2$  is the kinetic constant for the autocatalytic reaction ( $s^{-1}$ ), and  $m$  and  $n$  are the exponents of the kinetic model.

The exponent values depend on the reaction mechanism. When  $m = n = 1$ , the rate-determining step is a bimolecular reaction between a hydroxyl group and either amine group of an amine-epoxide species.<sup>38,39</sup> When  $m = 1$  and  $n = 2$ , it has been suggested that the rate-determining step is a trimolecular reaction among

TABLE II  
Kinetic Parameters Obtained by Linear Regression

$T$ (°C)	$k_1$ (s <sup>-1</sup> )	$n$	$k_2$ (s <sup>-1</sup> )	$r^2$
150	$1.34 \times 10^{-4}$	$n = 1$	$6.11 \times 10^{-4}$	0.913
180	$7.10 \times 10^{-4}$		$1.16 \times 10^{-3}$	0.724
	$E_1 = 88.6$ kJ/mol		$E_2 = 33.9$ kJ/mol	
150	$1.18 \times 10^{-4}$	$n = 2$	$1.05 \times 10^{-3}$	0.983
180	$5.68 \times 10^{-4}$		$3.42 \times 10^{-3}$	0.988
	$E_1 = 83.4$ kJ/mol		$E_2 = 62.8$ kJ/mol	

hydroxyl, amine, and epoxide groups.<sup>40,41</sup> Given the assumption that  $m = 1$ ,

$$\left(\frac{d\alpha}{dt}\right) \frac{1}{(1-\alpha)^n} = k_1 + k_2\alpha \quad (2)$$

The integration of eq. (1) led to the following expressions at the most common  $n$  values:

$$t = \frac{1}{(k_1 + k_2)} \ln \frac{\left(1 + \frac{k_2}{k_1}\alpha\right)}{(1-\alpha)} \quad n = 1 \quad (3)$$

$$t = \frac{1}{(k_1 + k_2)} \left[ \frac{k_2}{k_1 + k_2} \ln \frac{\left(1 + \frac{k_2}{k_1}\alpha\right)}{(1-\alpha)} + \frac{\alpha}{(1-\alpha)} \right] \quad n = 2 \quad (4)$$

By means of linear regression of eq. (2), it was possible to evaluate the rate constants  $k_1$  and  $k_2$  for different values of  $n$ . Table II contains the kinetic parameters thus calculated as well as the activation energy for both the nonautocatalytic and autocatalytic reactions. At both temperatures the autocatalytic reaction was faster than the nonautocatalytic reaction. In contrast, the kinetic constants at 180°C were 2–5 times higher than those at 150°C. Moreover, the activation barriers for the autocatalytic reaction ( $E_2 = 33.9$  and 62.8 kJ/mol for  $n = 1$  and  $n = 2$ , respectively) were lower than those for the nonautocatalytic reaction ( $E_1 = 88.6$  and 83.4 kJ/mol for  $n = 1$  and  $n = 2$ , respectively). The best results were obtained for the trimolecular reaction (i.e.,  $m = 1, n = 2$ ) as evidenced by analysis of variance and regression coefficients. Once the kinetic parameters were evaluated, it was possible to recalculate the conversion as a function of time from eqs. (3) and (4) for  $n = 1$  and  $n = 2$ , respectively. Figure 7 illustrates the comparison between experimental and theoretical conversion at 180°C for  $m = 1$  and  $n = 2$  (i.e., the best kinetic model). Within the entire conversion interval, the experimental and theoretical values were quite

similar (i.e., differences as low as 2–3%). Figure 8 shows the reaction rate of the curing at 180°C. Again, the autocatalytic model for  $m = 1$  and  $n = 2$  was in very good agreement with the experimental data. The maximum reaction rate at 180°C was 5.0%/min whereas this value at 150°C was 1.3%/min (i.e., 3.9 times lower). Finally, the adjustment of the experimental data to an  $n$ -order kinetic model was very poor and physically incongruous because the reaction order calculated was negative.

## CONCLUSIONS

Total curing of epoxy resins is produced after 7 h at 200°C. It is independent of the curing cycle that is used because, in both cases, the IR spectra obtained show the total consumption of both primary amine and epoxide groups. Therefore, curing cycle 2 proposed in this work is preferable and economical because it arrives at the same results as curing cycle 1 and saves significant operation time. The evolution of the curing process was followed by quantifying the changes that

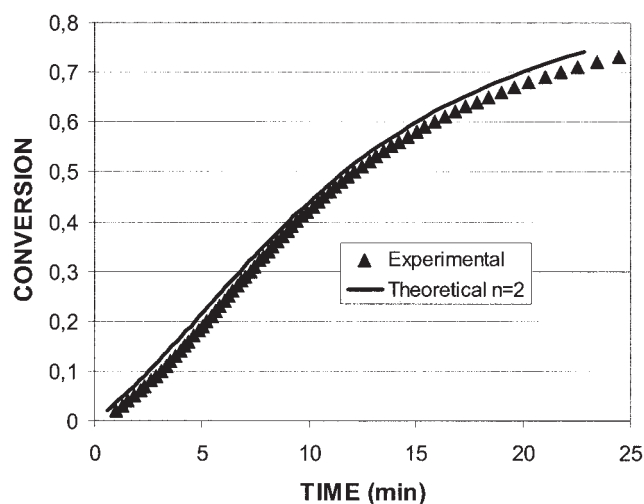
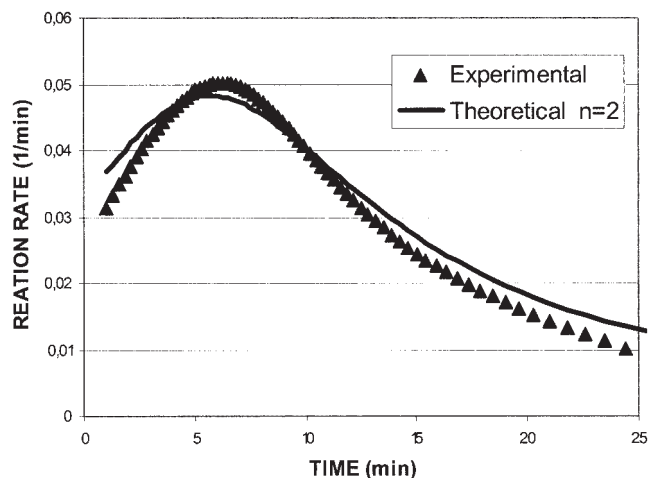


Figure 7 A comparison of the experimental and theoretical (autocatalytic kinetic model,  $m = 1, n = 2$ ) conversions at 150 and 180°C.



**Figure 8** A comparison of the experimental and theoretical (autocatalytic kinetic model,  $m = 1$ ,  $n = 2$ ) reaction rates at 150 and 180°C.

occur in particular bands of the IR spectra at different time periods. These bands basically correspond to amine groups (primary and secondary) and to epoxide groups. The curing cycle selected influences the evolution of the curing process as seen by the consumption relationship between epoxide and primary amine groups. Through DSC it was possible to evaluate the total enthalpy of the curing process and the glass-transition temperature of the system that was studied, showing that the latter greatly depends on temperature. The enthalpy measurements allowed the thermal conversion of the curing process to be calculated at different temperatures, and this conversion increased when increasing the temperature of the curing process. A higher curing temperature likewise implies that the resin reaches the vitrification point in less time. The autocatalytic kinetic model was able to adequately represent the experimental data. The best results were obtained when the rate-determining step was a trimolecular reaction ( $m = 1$ ,  $n = 2$ ), being  $k_1 = 1.18 \times 10^{-4} \text{ s}^{-1}$  and  $k_2 = 1.05 \times 10^{-3} \text{ s}^{-1}$  at 150°C and  $k_1 = 5.68 \times 10^{-4} \text{ s}^{-1}$  and  $k_2 = 3.42 \times 10^{-3} \text{ s}^{-1}$  at 180°C. The activation energies for the nonautocatalytic and autocatalytic reactions were 83.4 and 62.8 kJ/mol, respectively. The maximum conversion rates were 1.3 and 5.0%/min at 150 and 180°C, respectively.

## References

1. Mark, H.; Bikales, N.; Overberger, Ch.; Menges, G.; Kroschwitz J. Encyclopedia of Polymer Science and Engineering; Wiley: New York, 1985; Vol. 6.
2. Mustata, F.; Bicu, F. J Appl Polym Sci 2000, 77, 2430.

3. Lee, H.; Neville, K. Epoxy Resins. Their Applications and Technology; McGraw-Hill: New York, 1957.
4. Plazcek, D. J.; Frund, Z. N. J Polym Sci Part B: Polym Phys 1990, 28, 431.
5. Turi, E. Thermal Characterization of Polymeric Materials, 2nd ed.; Academic: San Diego, CA, 1997; Vol. 2.
6. Bonnaud, L.; Pascault, J. P.; Sauterau, H. Eur Polym J 2000, 36, 1313.
7. Xiao, J.; Delamar, M.; Shannahan, M. J Appl Polym Sci 1997, 65, 449.
8. Mijovic, J.; Fishbain, A.; Wijaya, J. Macromolecules 1992, 25, 979.
9. Montserrat, S.; Flaqué, C.; Pagès, P.; Málek, J. J Appl Polym Sci 1995, 56, 1413.
10. Gao, J.; Li, L.; Deng, Y.; Gao, Z.; Xu, C.; Zhang, M. J Therm Anal 1997, 49, 303.
11. Min, B. G.; Stachurski, Z. H.; Fodgkin, J. H. Polymer 1993, 34, 4488.
12. Salla, J.; Ramis, X. J Appl Polym Sci 1994, 51, 453.
13. Musto, P.; Martuscelli, E.; Ragosta, G.; Russo, P.; Villano, P. J Appl Polym Sci 1999, 74, 532.
14. Opalicki, M.; Kenny, J. M.; Nicolais, L. J Appl Polym Sci 1996, 61, 1025.
15. Varley, R. J.; Hodgkin, J. H.; Hawthorne, D. G.; Simon, G. P. J Appl Polym Sci 1996, 60, 2251.
16. Evans, A.; Williams, S.; Beaumont, P. J Mater Sci 1985, 20, 3668.
17. Stevens, G. J Appl Polym Sci 1981, 26, 4259.
18. Morgan, R.; Mones, E. J Appl Polym Sci 1987, 33, 999.
19. Nigel, St.; Graeme, G. Polymer 1992, 33, 2679.
20. Xu, L.; Schlup, J. J Appl Polym Sci 1998, 67, 895.
21. Morgan, R.; Kong, F. M.; Walkup, C. Polymer 1984, 25, 375.
22. Lachenal, G.; Pierret, A.; Poisson, N. Micron 1996, 27, 329.
23. Varley, R. J.; Heath, G. R.; Hawthorne, D. G.; Hodgkin, J. H.; Simon, G. P. Polymer 1995, 36, 1347.
24. Musto, P.; Ragosta, G.; Russo, P.; Mascia, L. Macromol Chem Phys 2001, 202, 3445.
25. Maddanimath, T.; Kholam, Y. B.; Aslam, M.; Mulla, I. S.; Vijayamohan, K. J Powder Sources 2003, 124, 133.
26. Bellenger, V.; Verdu, J.; Francillette, J.; Hoarau, P.; Morel, E. Polymer 1987, 28, 1079.
27. George, G. A.; Cash, G. A.; Rintoul, L. Polym Int 1996, 41, 169.
28. Meyer, F.; Sanz, G.; Eceiza, A.; Mondragón, I.; Mijovic, J. Polymer 1995, 36, 1407.
29. Musto, P.; Martuscelli, E.; Ragosta, G.; Russo, P.; Scarinzi, G. J Appl Polym Sci 1998, 69, 1029.
30. Bikales, N.; Overberger, Ch.; Menges, G.; Kroschwitz, J. Encyclopedia of Polymer Science and Engineering; Wiley: New York, 1985; Vol. 4.
31. Min, B. G.; Stachurski, Z. H.; Hodgkin, J. H.; Heath, G. R. Polymer 1993, 34, 3620.
32. Gupta, A.; Cizmecioglu, M.; Coulter, D.; Liang, R. H.; Yavrouian, A.; Tsay, F. D.; Moacanin, J. J Appl Polym Sci 1983, 28, 1011.
33. Kim, B. S.; Inoue, T. Polymer 1995, 36, 1985.
34. Woo, E.; Seferis, J. J Appl Polym Sci 1990, 40, 1237.
35. MacKinnon, A.; Jenkins, S.; McGrail, P.; Pethrick, R. Macromolecules 1992, 25, 3492.
36. White, S.; Mather, P.; Smith, M. Polym Eng Sci 2002, 42, 51.
37. Montserrat, S. J Appl Polym Sci 1992, 44, 545.
38. Zukas, W. X.; Schneider, N. S.; MacKnight, W. J Polym Mater Sci Eng 1983, 49, 588.
39. Enikolopiyan, N. S. Pure Appl Chem 1976, 48, 317.
40. Horie, K.; Hiura, H.; Sawada, M.; Mita, I.; Kambe, H. J Polym Sci Part A-1 1970, 8, 135.
41. Smith, I. T. Polymer 1961, 2, 95.